Atmos. Chem. Phys. Discuss., 9, 4691–4725, 2009
www.atmos-chem-phys-discuss.net/9/4691/2009/
© Author(s) 2009. This work is distributed under
the Creative Commons Attribution 3.0 License.

Atmospheric Chemistry and Physics Discussions

This discussion paper is/has been under review for the journal *Atmospheric Chemistry and Physics (ACP)*. Please refer to the corresponding final paper in *ACP* if available.

Impacts of aerosol indirect effect on past and future changes in tropospheric composition

N. Unger[1,2], **S. Menon**[3], **D. T. Shindell**[1], **and D. M. Koch**[1]

[1]NASA Goddard Institute for Space Studies, New York, NY, USA
[2]Columbia University, New York, NY, USA
[3]Lawrence Berkeley National Laboratory, Berkeley, CA, USA

Received: 20 January 2009 – Accepted: 22 January 2009 – Published: 24 February 2009

Correspondence to: N. Unger (nunger@giss.nasa.gov)

Published by Copernicus Publications on behalf of the European Geosciences Union.

Abstract

The development of effective emissions control policies that are beneficial to both climate and air quality requires a detailed understanding of all the feedbacks in the atmospheric composition and climate system. We perform sensitivity studies with a global atmospheric composition-climate model to assess the impact of aerosols on tropospheric chemistry through their modification on clouds, the aerosol indirect effect (AIE). The model includes coupling between both tropospheric gas-phase and aerosol chemistry and aerosols and liquid-phase clouds. We investigate past impacts from preindustrial (PI) to present day (PD) and future impacts from PD to 2050 (for the moderate IPCC A1B scenario) that embrace a wide spectrum of precursor emission changes and consequential aerosol-cloud interactions. The AIE is estimated to be $-2.0\,\mathrm{W\,m^{-2}}$ for PD–PI and $-0.6\,\mathrm{W\,m^{-2}}$ for 2050–PD, at the high end of current estimates. Inclusion of aerosol-cloud interactions substantially impacts changes in global mean methane lifetime across both time periods, enhancing the past and future increases by 10% and 30%, respectively. In regions where pollution emissions increase, inclusion of aerosol-cloud effects leads to 20% enhancements in in-cloud sulfate production and ~10% enhancements in sulfate wet deposition that is displaced away from the immediate source regions. The enhanced in-cloud sulfate formation leads to larger increases in surface sulfate across polluted regions (~10–30%). Nitric acid wet deposition is dampened by 15–20% across the industrialized regions due to AIE allowing additional re-release of reactive nitrogen that contributes to 1–2 ppbv increases in surface ozone in outflow regions. Our model findings indicate that aerosol-cloud interactions must be considered in studies of methane trends and projections of future changes to particulate matter air quality.

ACPD

9, 4691–4725, 2009

1 Introduction

Chemistry-aerosol-climate interactions represent one of the most important and most difficult foci of global change research. On the one hand, a significant part of the current human-made radiative forcing occurs through chemically active species, the most important of which are tropospheric ozone (O_3) and fine aerosol particles including sulfate, black carbon (BC) and organic carbon (OC). On the other hand, changes in climate can lead to changes in the chemical composition of the atmosphere both by altering emissions and through changes in the chemical processes that occur in the atmosphere. Furthermore, coupling between gas and aerosol systems, especially O_3 and sulfate can influence both composition and climate change (Unger et al., 2006a).

The direct effects of aerosols on global and regional tropospheric composition have been reasonably well studied (e.g. Dentener et al., 1993; Tie et al., 2003; Martin et al., 2003; Liao and Seinfeld, 2005). In general, aerosols have large and significant impacts on O_3 and oxidation capacity, especially in polluted regions, usually acting to suppress photochemistry by decreasing available photochemically active radiation and providing surfaces for heterogeneous reaction processes. It is essential to include such effects of aerosols in global atmospheric chemistry models in order to reconcile simulations of O_3 and precursors with observations. In contrast, the radiative effects of clouds on tropospheric photochemistry on the global average have been found to be only modest, the dominant effect being to influence the vertical redistribution of the intensity of photochemical activity (Liu et al., 2006). To our knowledge, the impact of aerosols on tropospheric chemistry through their modification on clouds remains poorly quantified. A recent model study found that the aerosol-induced cloud changes for the near future 2030 to present day time period may decrease O_3 forcing by up to 20% globally (Menon et al., 2008a). Therefore such cloud-aerosol-chemistry interactions warrant further examination.

The influence of aerosols on clouds, the "aerosol indirect effect" (AIE), is usually split into two effects: (a) the first aerosol indirect effect: increased (decreased) cloud

ACPD
9, 4691–4725, 2009

reflectivity due to an increase (decrease) in aerosols and cloud droplet number concentrations (CDNC) and reduced (increased) droplet sizes for the same liquid water content (LWC) (Twomey, 1991); and (b) the second aerosol indirect effect: change in cloud cover (CC), cloud liquid water path (LWP) and precipitation due to smaller droplet sizes that inhibit precipitation processes, thereby increasing CC and LWP (and thus cloud optical depths) (Albrecht, 1989). These aerosol-cloud interactions may influence photochemistry and composition through several pathways. Changes to available radiation fields may impact photolysis frequencies and changes to cloud lifetime and precipitation may alter rates of in-cloud processing and wet deposition of pollutants and precursors. In turn, all of these cloud effects on chemistry will influence O_3, sulfate and methane (CH_4) lifetime. The overall impact of the AIE on composition is complex due to effects of competing sign and cannot be determined without a 3-dimensional global model that includes all processes and feedbacks interactively.

We apply a state-of-the-art global atmospheric composition and climate model to simulate three time periods: preindustrial (PI), present day (PD) and a future world at 2050. For each time slice, two simulations are performed: the first includes an interactive treatment of the AIE (allowing CDNC to change with changing aerosol concentrations) and the second uses fixed CDNC. With fixed CDNC, cloud droplet size and optical properties are mainly dependent on cloud condensate, whereas for the interactive AIE treatment, both CDNC and cloud condensate determine cloud droplet size and cloud optical properties. Differences between the sensitivity simulations provide assessment of the impact of AIE on composition. The PD–PI change (labeled "past") features a large increase in anthropogenic aerosol loading across the polluted northern hemisphere and therefore substantial aerosol-cloud effects. For the 2050 future projection, the IPCC SRES A1B emissions scenario is selected. The 2050–PD change (labeled "future") features more complex regional shifts in gas and aerosol precursor emissions, and consequently aerosol-cloud interactions, with decreases at northern hemisphere mid-latitudes and increases in subtropical developing regions. The 2050 A1B scenario has already been the focus of chemistry-climate studies that have in-

ACPD
9, 4691–4725, 2009

vestigated the climate response due to O_3 and aerosol pollution (Shindell et al., 2007) and future changes to surface air quality over the US (Wu et al., 2008). Here, we extend these previous analyses by probing the role of aerosol-induced cloud changes in affecting the composition.

The goal of this study is to quantify the impacts of aerosol-cloud interactions on tropospheric chemistry and composition for past and future changes where there are substantial changes in aerosol loading. The development of effective emissions control policies that are beneficial to both climate and air quality requires a detailed understanding of all the feedbacks in the atmospheric composition and climate system. In Sect. 2 we describe the methodology including: Atmospheric composition-climate model (2.1), Emissions (2.2) and Simulations (2.3). In Sect. 3 we present analysis of the simulation results including: Aerosol distributions and impacts on cloud properties (3.1), Radiative forcing and AIE (3.2), $J(O^1D)$ photolysis rate (3.3), Zonal mean OH and global mean CH_4 lifetime (3.4), Sulfate in-cloud production and wet deposition (3.5), and O_3 and sulfate surface air quality (3.6). In Sect. 4 we present conclusions and recommendations.

2 Methodology

2.1 Atmospheric composition-climate model description

We applied the NASA Goddard Institute for Space Studies (GISS) model for Physical Understanding of Composition-Climate INteractions and Impacts (G-PUCCINI) described in detail and comprehensively evaluated in Shindell et al. (2006). The model comprises the GISS version ModelE general circulation model (Schmidt et al., 2006) with embedded fully interactive photochemistry and aerosol modules. The version used here includes sulfate, BC, OC and sea salt with coupling between the gas-phase chemistry and sulfate aerosol modules (Bell et al., 2005). The direct instantaneous top-of-the-atmosphere (TOA) radiative forcing by the short-lived pollutants (O_3, sulfate, BC

ACPD
9, 4691–4725, 2009

and OC) is calculated internally within the climate model's radiation scheme (Schmidt et al., 2006). The aerosols are assumed to be externally mixed. Additional details on optical and radiative schemes are provided in Koch et al. (2006). The schemes used to treat the AIE, coupling between aerosols and cloud microphysics for liquid-phase stratus and cumulus clouds, are described in detail in Menon and Rotstayn (2006). Essentially, separate relationships are used to describe the coupling between aerosols and liquid-phase stratiform and convective clouds. Aerosol mass concentrations are converted to aerosol number concentrations assuming log-normal distributions and are related to CDNC through empirical equations. Additionally, effects of changes to cloud cover and turbulence on CDNC are also included. To represent aerosol effects on precipitation, the autoconversion scheme in the model is modified to include a dependence on droplet size (as well as CDNC and droplet dispersion effects) such that autoconversion is triggered if droplet sizes exceed 14 µm as described in Rotstayn and Liu (2005). In the standard scheme, without aerosol-cloud interactions, autoconversion is an increasing function of cloud condensate. The AIE is estimated based on the difference in net cloud radiative forcing between time periods (Menon et al., 2002).

We use 23 vertical layers (model top in the mesosphere) and 4×5 degree latitudinal by longitudinal horizontal resolution. Chemical calculations are performed only in the troposphere in the present version of the model. We use a thermal tropopause defined by the meteorological lapse rate. Stratospheric values of O_3, NO_x and CH_4 are prescribed according to satellite observations with seasonally varying abundances (Shindell et al., 2003). The model performance with respect to key short-lived tracers has been comprehensively evaluated for O_3, nitrogen species, and reduced carbon species (Shindell et al., 2006), CO (Shindell et al., 2005) and sulfate and sea salt aerosols (Koch et al., 2006) and carbonaceous aerosols (Koch et al., 2007). Tropospheric O_3 is well simulated, especially in the vicinity of the tropopause, where it has the greatest effect on climate, and at the surface, where is affects air quality, with an average bias of only 6% against a comprehensive ozonesonde dataset (Shindell et al., 2006). The tropospheric chemistry version of G-PUCCINI performed well in a recent

CC BY

multi-model intercomparison involving evaluation against ozonesonde climatology, with a root-mean-square (rms) error value of 6.3 ppbv compared with a range of rms error values of 4.6 to 17 ppbv (Stevenson et al., 2006). Comparisons of the vertical profiles of NO_x and nitric acid (HNO_3) show good agreement between the model and observations from a variety of aircraft measurements across many regions (Shindell et al., 2006). The model's simulation of CO has been compared extensively with both surface and satellite observations (Shindell et al., 2005). It shows good agreement in both magnitude and seasonality, suggesting that the model's hydroxyl radical fields are reasonably realistic. Monthly mean correlations against mid-tropospheric satellite observations from MOPITT (Measurements of Pollution in the Troposphere) were typically in the range of 0.8–0.9. The sulfate model is generally within a factor of 2 of observations (Koch et al., 2006). Model sulfate at remote sites is generally less than observed. Carbonaceous aerosols are also typically within a factor of 2 of surface concentration observations, but are underestimated by more than a factor of 5 in Southeast Asia.

Model simulated AIE effects have been evaluated with satellite-based retrievals to constrain the magnitude of the AIE (Menon et al., 2008b). Results indicate that the AIE may be over-predicted over the ocean regions due to an under-prediction of cloud droplet size and an over-prediction of cloud optical depth. Simulated CDNC was found to be within satellite retrieved uncertainty. Over land locations, coincident retrievals of aerosols and cloud properties are not easily available from satellites and thus evaluation of changes to cloud properties from aerosols is more difficult. Over some land locations such as the Arctic, model-simulated values of the CDNC have been found to be too large, compared to satellite-retrievals, though COD and effective radii were within the observed range (Menon et al., 2008a). A more meaningful global evaluation of the AIE is challenging in the absence of global observations of CDNC that serve as the main link between aerosols and cloud properties.

CC BY

2.2 Emissions

Table 1 indicates the trace gas and aerosol precursor emissions inventories used for the PD, PI and 2050 simulations. For PD, we used anthropogenic CO, NO_x, NMVOCs and SO_2 emissions from the Emissions Database for Global Atmospheric Research (EDGAR3.2) for the year 1995 (Olivier and Berdowski, 2001). BC and OC emissions are not available in the EDGAR3.2 database and we used values from another global inventory for the year 1996 (Bond et al., 2004). The emissions include all anthropogenic fossil fuel, biofuel and biomass sources. Natural precursor and aerosol emissions are prescribed according to conventional estimates detailed elsewhere (Unger et al., 2006b). The conventional approach to PI emissions is adopted. We switch off all anthropogenic fossil and biofuel emissions and reduce biomass burning to 10% of PD values. The 2050 A1B emissions scenario is described in further detail in Shindell et al. (2007).

2.3 Simulations

Two sensitivity simulations were run for each of three time periods: PD, PI and future 2050, described in Table 2. The first set of models runs: Sim PD_AIE, Sim PI_AIE, Sim 2050_AIE, include interactive treatment of aerosol-cloud coupling and AIE. The second set of model runs: Sim PD, Sim PI, Sim 2050, use fixed CDNC (60 cm^{-3} over ocean and 174 cm^{-3} over land).

For the PI, PD and 2050 simulations we use monthly mean sea surface temperatures and sea ice climatologies for 1876–1885 (Rayner et al., 2003), 1990–1999 (Rayner et al., 2003) and 2050–2059 (IPCC A1B scenario) (Hansen et al., 2007), respectively. Thus, both emission changes and physical climate change effects are included. Clouds will be affected by changes in both aerosol loading and changes in sea surface temperatures and both types will impact the chemistry. Our sensitivity study approach allows isolation of the impacts of the aerosol-induced cloud changes only on composition since both experiments in each time slice use the same sea surface temperature

ACPD
9, 4691–4725, 2009

and sea ice climatologies.

CH_4 concentrations used for the different time periods are included in Table 1. For PD and 2050 conditions, CH_4 concentration is prescribed to hemisphere average values that were generated in previous simulations with a similar model but using a fully interactive CH_4 cycle (Unger et al., 2006b; Shindell et al., 2007). For PI, CH_4 is fixed to the observed concentrations from ice core records.

All the simulations were run for 12 model years with the same emissions each year, but with GCM meteorological interannual variability; the first 2 years of the simulations are discarded as spin-up and the remaining 10 years are averaged for analysis.

3 Results

Differences between the two sensitivity simulations in the same time slice are dependent on the choice of fixed CDNC, therefore may be somewhat arbitrary. Our focus here is the impact of changing aerosol loading on clouds and feedbacks to composition across time periods. In order to isolate the impacts of past and future AIE on the change in a composition variable, we take the difference between the change in variable (X) between the two time periods for simulations that include AIE versus the simulations that do not include AIE e.g. [(Sim PD_AIE(X) – Sim PI_AIE(X)) – (Sim PD(X) – Sim PI(X))]. The significance of the difference is determined relative to the model's interannual meteorological variability over the 10 model run years. All areas shown in color (not white) on the figures are significant at the 95% confidence level.

3.1 Aerosol distributions and impacts on cloud properties

Table 3 shows the aerosol column densities for the time periods of interest. Human activities have led to a huge increase in aerosol loading in the atmosphere especially over polluted source regions. Globally, for the PD–PI change, there is a 100% increase in sulfate, 200% increase in OC and 2000% increase in BC, regional increases in

CC BY

polluted regions are more dramatic. The changes in aerosol loading are more complex for the future change. Sulfate loading increases by around 20% globally and 40% over East Asia, but decreases over North America (−20%) and Europe (−10%). BC loading decreases by −25% globally and by around −40% across all of the regions, mainly due to reductions in emissions from fossil and biofuel sources. Similarly, OC loading decreases globally and over Europe by −15% with larger decreases of up to −25% across North America and Asia. We do not dwell here on analysis of past and future changes in composition since these have been extensively examined previously in the GISS model for PD–PI (Shindell et al., 2003; Koch et al., 1999) and 2050–PD (Shindell et al., 2007; Koch et al., 2007).

The influences of the changes in human-made aerosol loading on cloud properties are indicated in Table 4. The PD–PI increases in global average CDNC, LWP and COD and coincident decrease in cloud droplet effective radius (R_{eff}) are consistent with prior studies using similar treatment of the AIE in the GISS model (Menon and Del Genio, 2007). As expected CC increased from PI to PD due to aerosol-cloud interactions. Without including aerosol-induced changes to clouds, CC decreases between PD and PI, due to climate-related changes that tend to decrease CC with increased GHG warming, as also found by Koch et al. (2009). Figure 1 shows the aerosol-induced changes in cloud properties between 2050–PD. Changes in CDNC are consistent with changes in aerosol concentrations. Areas where aerosol concentrations decrease (e.g. N. America, Europe) indicate a decrease in CDNC. Over East Asia and the biomass burning regions, CDNC increases due to an increase in aerosols (industrial over Asia and biomass for South America and Africa). Although COD increases/decreases in areas where CDNC increase/decrease, as expected, CC changes do not follow a similar pattern. For the PD–PI simulations, large changes in CDNC (~80%) result in an increase in total and low CC (0.13% and 0.18%, respectively), even though climate-related changes tend to decrease CC. For the future scenario, CDNC is approximately the same and thus CC changes are more determined by climate-related changes, as indicated by CC changes for simulations without the AIE. Menon et al. (2008b) found

ACPD
9, 4691–4725, 2009

that CC changes, due to aerosol-cloud interactions, were more strongly dependent on meteorological changes than on aerosol-induced changes. Similar effects are observed in these simulations. Thus, the AIE influence is relatively small for the future scenario as compared to the changes obtained for the past (PD–PI) simulations.

3.2 Radiative forcing and AIE

The resultant radiative forcings for the past (PD–PI) and future (2050–PD) time periods are included in Table 5 and the estimated AIE based on cloud radiative forcing is shown in Fig. 2. In this version of the model the past direct aerosol forcing is $-0.11\,W\,m^{-2}$ since the negative sulfate and positive BC forcings largely cancel each other out. We estimate the AIE by taking the difference in net cloud radiative forcing between time periods. The past AIE is $-2.0\,W\,m^{-2}$, higher than previous GISS model estimates (Menon et al., 2008a; Koch et al., 2009) and estimates based on constraints from the temperature record using a parameterized AIE treatment in a similar version of the GISS model (Hansen et al., 2005). However, changes in CDNC in the Koch et al. (2009) simulations are about half of that obtained in this study since the Koch et al. study used a different set of emissions that had a lower sulfate burden change. Thus, the AIE we obtain is high but within the range predicted by other studies that vary from 0.5 to $-2.0\,W\,m^{-2}$ for both indirect effects (Lohmann and Feichter, 2005). Forster et al. (2007) give a current best estimate of the range (-1.1 to $+0.4\,W\,m^{-2}$) and median value ($-0.70\,W\,m^{-2}$) from a multi-model assessment of the cloud albedo effect only. Our simulations include both indirect effects and are thus larger.

For the future scenario, where there are more complex spatial changes in aerosol loading, the net aerosol direct forcing is larger than for the past change by about a factor of two ($-0.18\,W\,m^{-2}$) because the carbonaceous aerosol direct forcings are so small, despite a sulfate direct forcing only around one third of the PD–PI effect. Consequently, there is an enhanced AIE for the future scenario of $-0.6\,W\,m^{-2}$. For the future scenario, since CDNC changes are rather negligible (as shown in Table 4), cloud droplet size actually increases by ~0.5 μm as opposed to the decrease obtained for the past changes.

ACPD
9, 4691–4725, 2009

COD, LWP and CC change by a very small amount for the future scenario, and may be more influenced by climate-related changes. Thus, the indirect effect is weaker for the future scenario.

The effects of including AIE on past and future global annual mean forcings are small (Table 5) and appear largely negligible for past changes. In the future case, where pollution emissions are shifted to lower latitudes with higher insolation, inclusion of AIE reduces the magnitude of the sulfate direct forcing, and as a result the net aerosol direct forcing, by ~8%. This reduction in sulfate forcing is driven by enhanced in-cloud sulfate formation when aerosol-cloud interactions are included in the model. Sulfate formed in aqueous phase has a shorter lifetime and smaller impact on radiative forcing (e.g. Koch et al., 1999). The effect is more pronounced for precursor emissions increases at subtropical latitudes rather than for the past change when the emissions increases occurred at higher latitudes.

3.3 $J(O^1D)$ photolysis rate

The impact of AIE on the past (PD–PI) and future (2050–PD) changes in $J(O^1D)$ at the surface, important for O_3 air quality, are shown in Fig. 3. For the PD–PI change, the AIE supplements the decrease in $J(O^1D)$ across large regions of the globe. The AIE impacts the PD–PI change by about 50% across the eastern US, 80% across East Asia and across Europe, the AIE impacts dominate over the PD–PI change. The effects of the future AIE on the change in $J(O^1D)$ are found to be insignificant across North America and Europe since the aerosol loading changes are modest for the scenario that we examine. However, the suppression of $J(O^1D)$ due to increased AIE is evident across the Middle East and South Asian regions (~50–100% of 2050–PD change).

The effect on O_3 of a decrease in the $J(O^1D)$ photolysis channel depends on the background NO_x concentration. Under low NO_x conditions, a decrease in $J(O^1D)$ can induce increases in O_3 levels. Under more polluted photochemically active regions, the opposite may be true since this chain initiation process also drives the production

ACPD
9, 4691–4725, 2009

of O_3. The net impact of AIE on past and future surface O_3 changes is discussed in Sect. 3.6.

Since the $J(O^1D)$ photolysis channel is the major source of OH, there are corresponding decreases in the surface OH change (∼−20%) over polluted regions due to the AIE effects that somewhat counteract the general increase in surface OH fields for the PD–PI time period due to NO_x emissions increases (not shown). In the next section, we discuss the impacts of AIE on OH changes throughout the troposphere.

3.4 Zonal mean OH and global mean CH_4 lifetime

Figure 4 shows the impact of AIE on past and future changes in annual zonal mean OH throughout the troposphere. The model PD–PI change in OH is discussed in more detail in Shindell et al. (2003). Briefly, the PD–PI change features lower tropospheric OH increases in Northern Hemisphere tropical to mid-latitudes due to NO_x emissions increases at the surface, and more broad decreases in OH levels throughout the free troposphere due to increases in carbon monoxide (CO), CH_4 and non-methane volatile organic compounds (NMVOC) emissions. Inclusion of the AIE acts to amplify these changes further on the order of ∼10%. The largest AIE impact (∼−30%) on the OH change is in the middle and upper tropical troposphere where CH_4 oxidation is important. The suppression in $J(O^1D)$ photolysis rates in the lower troposphere due to enhanced AIE (Fig. 2) leads to reduced OH production and therefore decreased oxidation rates near the surface, allowing greater vertical transport of CO and NMVOC precursors to the middle and upper troposphere. In consequence, the OH in this region is decreased further for the PD–PI change when AIE effects are considered. The impacts of AIE on the 2050–PD change in OH follow a broadly similar pattern but shifted to lower latitudes in keeping with the precursor emissions shift, but are weaker (only a few percent at most) than past impacts.

The global mean CH_4 lifetime for each simulation and time period is shown in Table 6.

At all 3 time periods the influence of including interactive AIE in the model is to reduce the global mean CH_4 lifetime by about 2–3% relative to simulations that do not

ACPD
9, 4691–4725, 2009

include aerosol-cloud interactions in the same time slice. Global mean CH_4 lifetime increases from PI to PD and to a lesser extent from PD to 2050 due to increases in emissions of CO and other NMVOCs that compete with CH_4 for OH reaction, and increases in emissions of CH_4 itself, despite co-increases in NO_x emissions that tend to recycle OH radicals and decrease the CH_4 lifetime. Inclusion of AIE enhances the past and future increases in CH_4 lifetime by about 10% (1.1 versus 1.0 years) for the past case and 30% for the future case (0.21 versus 0.16 years). A previous model study attributed the observed decline in the CH_4 growth rate between 1990 and 2004 to a 1.6% reduction in the CH_4 lifetime (0.17 years) mainly due to OH increases driven by increases in lightning NO_x (Fiore et al., 2006). The substantial response of the change in CH_4 lifetime to AIE found here suggests that changing aerosol-cloud effects may play a significant role in influencing the CH_4 lifetime and need to be considered in studies of CH_4 trends.

3.5 Sulfate in-cloud production and wet deposition

The influences of AIE on the change in sulfate in-cloud production, wet deposition and HNO_3 wet deposition are shown in Fig. 5 (past) and Fig. 6 (future). Inclusion of AIE in the PD–PI case drives larger increases in in-cloud sulfate production across polluted regions where there have been aerosol-induced increases in CDNC, LWP and COD. This enhancement in sulfate production in clouds amounts to around 15–20% of the PD–PI change across eastern US and East Asia ($\sim$+50–100 mg m^{-2} yr^{-1}) due to AIE effects alone. At the same time, the effect of the AIE is to push precursor washout away from source regions as indicated for sulfate and HNO_3 in Figs. 5 and 6. In the immediate location of the pollution sources in the eastern US and China, the AIE appears to drive decreases in sulfate wet deposition that represent only 5–10% of the PD–PI change. In response to the enhanced in-cloud production, there are AIE-driven increases in sulfate wet deposition further north of the source regions and across Europe ($\sim$+50–100 mg m^{-2} yr^{-1}). The PD–PI increase in HNO_3 wet deposition rate is dampened due to AIE effects up to 10–15% across polluted source regions

ACPD
9, 4691–4725, 2009

(∼−100 mg m^{-2} yr^{-1}). Unlike for sulfate aerosol, if the HNO_3 lifetime with respect to washout is lengthened, the HNO_3 may be photolyzed such that the reactive nitrogen is re-released and available to participate in O_3 photochemistry. A corollary is that the notorious acid deposition problem due to industrialization in the past century in the northern forests across Europe and northeastern US was made worse by the AIE in the case of sulfate but lessened by the AIE in the case of HNO_3.

For the future 2050 A1B scenario that we examine, the projected decreases in aerosol-loading and AIE over North America and Europe are only modest and correspondingly the model suggests weaker impacts than for the past change on precursor washout and sulfate in-cloud production in these regions (Fig. 6). There is a dampening of in-cloud sulfate production across the US and movement of HNO_3 wet deposition back to the source regions due to AIE effects on the 2050–PD change that amounts to around 10% of the future change. AIE driven enhancements in in-cloud sulfate production (∼+20% of future change) are localized in source regions along the northeastern African coastline. Large and significant effects occur over Africa, the Middle East and South Asia where there are large increases in SO_2 emissions and thus aerosol loading. Fossil fuel and biofuel aerosol-driven increases in CDNC and COD in Central Africa cause marked dampening (∼−20% of the 2050–PD change) in the local wet deposition of sulfate and HNO_3, which is displaced across the Middle East and South Asian regions where there are enhancements up to 50–100% of the future change due entirely to AIE effects. This AIE-driven displacement of acid deposition adds new dimensions and complications to transboundary pollution problems.

3.6 O_3 and sulfate surface air quality

The resultant AIE effects on annual average surface O_3 and sulfate for the past and future changes are complex (Fig. 7). Enhanced AIE for the PD–PI change leads to enhanced surface O_3 in outflow regions from the major industrialized continental areas (western Europe, western Atlantic, western Pacific) that is about 1–2 ppbv or up to 10–

CC BY

20% of the past change on the annual average. This effect on surface O_3 is driven by two factors: (1) suppression of surface level $J(O^1D)$ which is a sink for O_3 under low NO_x conditions (2) displacement of precursor washout, e.g. HNO_3 that increases the availability of NO_x radicals for O_3 formation. A more quantitative attribution is difficult due to unavailability of reaction rate diagnostics in these particular model simulations. Tropospheric O_3 is well known to be highly buffered and relatively robust to perturbation. A recent multi-model intercomparison study found that 20% decreases in all O_3 precursors across major source regions exerted at most a ~1 ppbv decrease in local surface O_3 (Fiore et al., 2008). The AIE impacts on surface O_3 changes are therefore comparable to, or larger than, the impact of 20% reductions in all local O_3 precursor emissions.

Similarly, for the 2050–PD change, enhanced AIE drives an increase in surface O_3 change in the outflow region from South Asia, representing about 50% of the future change there. The 2050 A1B scenario projects only modest decreases in aerosol loading over North America and Europe relative to PD. Hence, there are only relatively weak AIE impacts on the future O_3 change over these regions for this particular emissions scenario (<0.5 ppbv). Other future scenarios that project more aggressive reductions in precursor emissions at these latitudes would likely have larger impacts on O_3 through aerosol-induced cloud changes (e.g. IPCC SRES B1, B2).

Past enhancements in AIE drive increases in surface sulfate that are about 10–20% of the PD–PI change across the eastern US, and up to ~20% across northern Europe and South East Asia, due to local increases in in-cloud production. For the future case, where AIE is diminished over the eastern US, there are further decreases in surface sulfate up to 50% of the 2050–PD change. The future AIE drives significant surface sulfate enhancements in tropical latitudes over western Africa and South East Asia (~20% of the future increase). Our model findings suggest that simulation of future changes to particulate air quality must include AIE.

ACPD
9, 4691–4725, 2009

4 Discussion and conclusions

We performed sensitivity studies with a global atmospheric composition-climate model to assess the impact of aerosols on tropospheric chemistry through their modification on clouds, the aerosol indirect effect (AIE). The model includes coupling between aerosol and O_3 chemistry and aerosols and liquid-phase clouds. The time periods that we considered are preindustrial to present day (past) and present day to 2050 (future). The model simulated AIE is $-2.0\,W\,m^{-2}$ for PD–PI and $-0.6\,W\,m^{-2}$ for 2050–PD. To our knowledge, this is the first global modeling assessment of AIE impacts on changes in CH_4 lifetime, in-cloud sulfate production and precursor wet deposition, and surface ozone and sulfate air quality.

Inclusion of aerosol-cloud interactions substantially impacts changes in global mean CH_4 lifetime across both time periods, enhancing the past and future increases by 10% and 30%, respectively. Inclusion of aerosol-cloud interactions has only subtle effects on global annual mean O_3 and aerosol direct radiative forcing, except for sulfate forcing in the future case, which is reduced by ~8% when AIE is included. More generally, including AIE in the past and future changes has only small impacts on global scales but large and significant effects on regional composition.

In regions where pollution emissions increase, inclusion of aerosol-cloud effects leads to 20% enhancements in the increases in in-cloud sulfate production. Sulfate wet deposition is enhanced by a similar amount further north of source regions and HNO_3 wet deposition is dampened by 15–20% and displaced away from the source regions. The enhanced in-cloud sulfate formation leads to larger increases (~10–30%) in surface sulfate across polluted regions. For the future case when precursor emissions are reduced over the eastern US, diminished AIE further reduces the surface sulfate change by ~50%. Impacts of AIE on surface O_3 changes are on the order of 1–2 ppbv increases in the outflow from polluted source regions (up to 10–20% of the PI to PD change). In our model, there is little net impact on surface the O_3 change between 2050 and PD over North America and Europe because the aerosol decreases

ACPD
9, 4691–4725, 2009

are relatively modest over these regions for the A1B scenario.

The results are dependent on the emissions scenarios that we have considered but may be extrapolated to serve as a guide to impact assessment for alternative projections. For example, future worlds with more aggressive aerosol reduction policies, or conversely with substantially greater aerosol emissions, will likely exert larger impacts on surface O_3, sulfate and CH_4 lifetime than found here.

The major limitations of the study are the large uncertainties associated with the AIE, partly driven by uncertainties in aerosol emission inventories, especially for carbonaceous aerosols, and the lack of available observations to assess aerosol-cloud feedbacks. At present it is challenging to provide observational constraints on aerosol-cloud impacts on composition. Next generation satellite data products may provide unprecedented insights into AIE and effects on composition.

Despite these shortcomings, our model sensitivity studies suggest that aerosol-cloud effects are an important feedback on regional-scale cloud processing, surface particulate matter and global scale CH_4 lifetime. Based on our model findings, we recommend that projections of future changes to particulate matter air quality and investigation of CH_4 trends must consider aerosol-cloud interactions.

Acknowledgements. We thank the NASA Atmospheric Chemistry Modeling and Analysis Program (ACMAP) for funding support. We thank the NASA Center for Computational Sciences for computing support.

References

Albrecht, B.: Aerosols, cloud microphysics, and fractional cloudiness, Science, 245, 1227, 1989.

Bell, N., Koch, D., and Shindell, D. T.: Impacts of chemistry-aerosol coupling on tropospheric ozone and sulfate simulations in a general circulation model, J. Geophys. Res., 110, D14305, doi:10.1029/2004JD005538, 2005.

Bond, T. C., Streets, D. G., Yarber, K. F., Nelson, S. M., Woo, J.-H., and Klimont, Z.:

A technology-based global inventory of black and organic carbon emissions from combustion, J. Geophys. Res., 109, D14203, doi:10.1029/2003JD003697, 2004.
Dentener, F. J. and Crutzen, P. J.: Reaction of N_2O_5 on tropospheric aerosols: impact on the global distributions of NO_x, O_3 and OH, J. Geophys. Res., 98, 7149–7163, 1993.
Fiore, A. M., Dentener, F. J., Wild, O., Cuvelier, C., Schultz, M. G., Hess, P., Textor, C., Schulz, M., et al.: Multi-model estimates of intercontinental source-receptor relationships for ozone pollution, J. Geophys. Res., doi:10.1029/2008jd010816, in press, 2008.
Fiore, A. M., Horowitz, L. W., Dlugokencky, E. J., and West, J. J.: Impact of meteorology and emissions on methane trends, 1990–2004, Geophys. Res. Lett., 33, L12809, doi:10.1029/2006GL026199, 2006.
Forster, P., Ramaswamy, V., Artaxo, P., et al.: Changes in atmospheric constituents and in radiative forcing, in: Climate Change 2007: The Physical Science Basis, 131–215, Cambridge Univ. Press, New York, 2007.
Hansen, J., Sato, M., Ruedy, R., et al.: Efficacy of climate forcings, J. Geophys. Res., 110, D18104, doi:10.1029/2005JD005776, 2005.
Hansen, J., Sato, M., Ruedy, R., Kharecha, P., Lacis, A., Miller, R., Nazarenko, L., Lo, K., Schmidt, G. A., Russell, G., Aleinov, I., Bauer, S., Baum, E., Cairns, B., Canuto, V., Chandler, M., Cheng, Y., Cohen, A., Del Genio, A., Faluvegi, G., Fleming, E., Friend, A., Hall, T., Jackman, C., Jonas, J., Kelley, M., Kiang, N. Y., Koch, D., Labow, G., Lerner, J., Menon, S., Novakov, T., Oinas, V., Perlwitz, Ja., Perlwitz, Ju., Rind, D., Romanou, A., Schmunk, R., Shindell, D., Stone, P., Sun, S., Streets, D., Tausnev, N., Thresher, D., Unger, N., Yao, M., and Zhang, S.: Dangerous human-made interference with climate: a GISS modelE study, Atmos. Chem. Phys., 7, 2287–2312, 2007, http://www.atmos-chem-phys.net/7/2287/2007/.
Koch, D., Jacob, D., Tegen, I., Rind, D., and Chin, M.: Tropospheric sulfur simulation and sulfate direct radiative forcing in the Goddard Institute for Space Studies general circulation model, J. Geophys. Res., 104, 23799–23822, doi:10.1029/1999JD900248, 1999.
Koch, D., Schmidt, G. A., and Field, C. V.: Sulfur, sea salt, and radionuclide aerosols in GISS ModelE, J. Geophys. Res., 111, D06206, doi:10.1029/2004JD005550, 2006.
Koch, D., Bond, T. C., Streets, D., Unger, N., and van der Werf, G.: Global impacts of aerosols from particular source regions and sectors, J. Geophys. Res., 112, D02205, doi:10.1029/2005JD007024, 2007.
Koch, D., Menon, S., Del Genio, A., Ruedy, R., Aleinov, I., and Schmidt, G. A.: Distinguishing

aerosol impacts on climate over the past century, J. Climate, in press, 2009.
Lohmann, U. and Feichter, J.: Global indirect aerosol effects: a review, Atmos. Chem. Phys., 5, 715–737, 2005, http://www.atmos-chem-phys.net/5/715/2005/.
Liao, H. and Seinfeld, J. H.: Global impacts of gas-phase chemistry-aerosol interactions on direct radiative forcing by anthropogenic aerosols and ozone, J. Geophys. Res., 110, D18208, doi:10.1029/2005JD005907, 2005.
Liu, H., Crawford, J. H., Pierce, R. B., Norris, P., Platnick, S. E., Chen, G., Logan, J. A., Yantosca, R. M., Evans, M. J., Kittaka, C., Feng, Y., and Tie, X.: Radiative effect of clouds on tropospheric chemistry in a global three-dimensional chemical transport model, J. Geophys. Res., 111, D20303, doi:10.1029/2005JD006403, 2006.
Martin, R. V., Jacob, D. J., Yantosca, R. M., Chin, M., and Ginoux, P.: Global and regional decreases in tropospheric oxidants from photochemical effects of aerosols, J. Geophys. Res., 108, 4097, doi:10.1029/2002JD002622, 2003.
Menon, S., Del Genio, A. D., Koch, D., and Tselioudis, G.: GCM simulations of the aerosol indirect effect: Sensitivity to cloud parameterization and aerosol burden, J. Atmos. Sci., 59, 692–713, doi:10.1175/1520-0469, 2002.
Menon, S. and Rotstayn, L.: The radiative influence of aerosol effects on liquid-phase cumulus and stratus clouds based on sensitivity studies with two climate models, Clim. Dynam., 27, 345–356, 2006.
Menon, S. and Del Genio, A. D.: Evaluating the impacts of carbonaceous aerosols on clouds and climate, in: Human-Induced Climate Change: An Interdisciplinary Assessment, edited by: Schlesinger, M. E., Kheshgi, H., Smith, J. B., de la Chesnaye, F. C., Reilly, J. M., Wilson, T., and Kolstad, C., Cambridge University Press, 34–48, 2007.
Menon, S., Unger, N., Koch, D., Francis, J., Garrett, T., Sednev, I., Shindell, D., and Streets, D.: Aerosol climate effects and air quality impacts from 1980 to 2030, Environ. Res. Lett., 3, 024004, doi:10.1088/1748-9326/3/2/024004, 2008a.
Menon, S., Del Genio, A. D., Kaufman, Y., Bennartz, R., Koch, D., Loeb, N., and Orlikowski, D.: Analyzing signatures of aerosol-cloud interactions from satellite retrievals and the GISS GCM to constrain the aerosol indirect effect, J. Geophys. Res., 113, D14S22, doi:10.1029/2007JD009442, 2008b.
Olivier, J. G. J. and Berdowski, J. J. M.: Global emissions sources and sinks, in: The Climate System, edited by: Berdowski, J., Guicherit, R., and Heij, B. J., 33–78, A. A. Balkema,

Brookfield, Vt, 2001.
Rayner, N. A., Parker, D. E., Horton, E. B., Folland, C. K., Alexander, L. V., Rowell, D. P., Kent, E. C., and Kaplan, A.: Global analyses of sea surface temperature, sea ice, and night marine air temperature since the late nineteenth century, J. Geophys. Res., 108(D14), 4407, doi:10.1029/2002JD002670, 2003.
Rotstayn, L. D. and Liu, Y.: A smaller global estimate of the second indirect aerosol effect, Geophys. Res. Lett., 32, L05708, doi:10.1029/2004GL021922, 2005.
Schmidt, G. A., Ruedy, R., Hansen, J. E., et al.: Present day atmospheric simulations using GISS ModelE: Comparison to in-situ, satellite and reanalysis data, J. Climate, 19, 153–192, 2006.
Shindell, D. T., Faluvegi, G., and Bell, N.: Preindustrial-to-present-day radiative forcing by tropospheric ozone from improved simulations with the GISS chemistry-climate GCM, Atmos. Chem. Phys., 3, 1675–1702, 2003, http://www.atmos-chem-phys.net/3/1675/2003/.
Shindell, D. T., Faluvegi, G., and Emmons, L. K.: Inferring carbon monoxide pollution changes from space-based observations, J. Geophys. Res., 110, D23303, doi:10.1029/2005JD006132, 2005.
Shindell, D. T., Faluvegi, G., Unger, N., Aguilar, E., Schmidt, G. A., Koch, D. M., Bauer, S. E., and Miller, R. L.: Simulations of preindustrial, present-day, and 2100 conditions in the NASA GISS composition and climate model G-PUCCINI, Atmos. Chem. Phys., 6, 4427–4459, 2006, http://www.atmos-chem-phys.net/6/4427/2006/.
Shindell, D. T., Faluvegi, G., Bauer, S. E., Koch, D., Unger, N., Menon, S., Miller, R. L., Schmidt, G. A., and Streets, D. G.: Climate response to projected changes in short-lived species under the A1B scenario from 2000–2050 in the GISS climate model, J. Geophys. Res., 112, D20103, doi:10.1029/2007JD008753, 2007.
Stevenson, D. S., Dentener, F. J., Schultz, M. G., et al.: Multimodel ensemble simulations of present-day and near-future tropospheric ozone, J. Geophys. Res., 111, D08301, doi:10.1029/2005JD006338, 2006.
Tie, X., Emmons, L., Horowitz, L., Brasseur, G., Ridley, B., Atlas, E., Stroud, C., Hess, P., Klonecki, A., Madronich, S., Talbot, R., and Dibb, J.: Effect of sulfate aerosol on tropospheric NO_x and ozone budgets: Model simulations and TOPSE evidence, J. Geophys. Res., 108(D4), 8364, doi:10.1029/2001JD001508, 2003.
Twomey, S. A.: Aerosols, clouds and radiation, Atmos. Environ., 25A, 2435–2442, 1991.

CC BY

Unger, N., Shindell, D. T., Koch, D. M., and Streets, D. G.: Cross influences of ozone and sulfate precursor emissions changes on air quality and climate, P. Natl. Acad. Sci., 103, 4377–4380, doi:10.1073pnas.0508769103, 2006a.

Unger, N., Shindell, D. T., Koch, D. M., Amann, M., Cofala, J., and Streets, D. G.: Influences of man-made emissions and climate changes on tropospheric ozone, methane and sulfate at 2030 from a broad range of possible futures, J. Geophys. Res., 111, D12313, doi:10.1029/2005JD006518, 2006b.

Wu, S., Mickley, L. J., Leibensperger, E. M., Jacob, D. J., Rind, D., and Streets, D. G.: Effects of 2000–2050 global change on ozone air quality in the United States, J. Geophys. Res., 113, D06302, doi:10.1029/2007JD008917, 2008.

Table 1. Total and anthropogenic precursor emissions of CO ($Tg\,yr^{-1}$), NO_x ($Tg\,N\,yr^{-1}$), NMVOC ($Tg\,C\,yr^{-1}$), SO_2 ($Tg\,S\,yr^{-1}$), BC ($Tg\,yr^{-1}$), OC($Tg\,yr^{-1}$) used in each time slice. Biomass burning is classified as anthropogenic. Prescribed CH_4 concentrations (ppbv) are also indicated.

Total Emission	PI	PD	2050 A1B
CO	30	847	1146
NO_x	13	46	77
NMVOC	579	707	759
SO_2	11	84	82
BC	0.4	8	6
OC	20	58	51
Anthropogenic Emission			
CO	30	847	1146
NO_x	0.4	33	65
NMVOC	2	132	192
SO_2	0.1	73	71
BC	0.4	8	6
OC	3	42	35
Prescribed CH_4 concentration			
Northern Hemisphere	790	1850	2932
Southern Hemisphere	790	1720	2780

ACPD
9, 4691–4725, 2009

Table 2. Description of simulations.

Name	Description	Emissions	Climate	AIE
Sim PD_AIE Sim PD	Present day	1995	1990s	ON OFF
Sim PI_AIE Sim PI	Preindustrial	~1850	1880s	ON OFF
Sim 2050_AIE Sim 2050	Future 2050	2050	2050s	ON OFF

ACPD
9, 4691–4725, 2009

Table 3. Aerosol column densities for the simulations with aerosol-cloud interactions included for the global domain and key source regions.

Domain and time slice	Sulfate (mg m^{-2})	BC (mg m^{-2})	OC (mg m^{-2})
Global			
PI	1.43	0.014	0.58
PD	2.93	0.31	1.91
2050A1B	3.48	0.23	1.6
North America			
PI	1.35	0.007	0.847
PD	5.40	0.383	2.04
2050A1B	4.36	0.23	1.51
Europe			
PI	1.50	0.004	0.554
PD	5.37	0.43	1.55
2050A1B	4.83	0.26	1.3
East Asia			
PI	0.89	0.009	0.555
PD	3.96	0.637	2.38
2050A1B	5.70	0.37	1.77

ACPD
9, 4691–4725, 2009

Table 4. Global and regional average cloud variables for the simulations with aerosol-cloud interactions included. Results for simulations without aerosol-cloud interactions are in brackets. In the simulations without aerosol-cloud interactions switched on, CDNC is fixed to 60 cm^{-3} over ocean and 174 cm^{-3} over land. For cloud cover (CC), values for both total and low CC are indicated.

Domain and time slice	CNDC (cm^{-3})	Reff (μm)	LWP (g/m^2)	COD	Total CC (%)	Low CC (%)
Global						
PI	80.7	21.5	59 (83)	10.3 (15.2)	64.61 (65.05)	54.34 (54.62)
PD	145.6	20.7	63 (84)	13.1 (15.2)	64.74 (64.78)	54.52 (54.30)
2050A1B	150.0	21.2	66 (87)	13.32 (15.5)	65.07 (65.21)	55.03 (54.91)
North America						
PI	58.8	17.3	44 (73)	11.4 (20.0)	51.52 (52.25)	39.49 (40.02)
PD	221.4	16.0	54 (74)	19.4 (20.0)	52.70 (53.20)	40.72 (40.86)
2050A1B	200.3	18.3	60 (88)	18.2 (20.7)	55.86 (56.74)	44.53 (45.16)
Europe						
PI	68.3	18.0	41 (73)	9.9 (17.6)	68.27 (70.32)	59.21 (61.70)
PD	245.5	16.5	56 (74)	16.2 (17.7)	69.26 (69.70)	60.48 (60.70)
2050A1B	174.5	16.3	51 (76)	14.9 (19.0)	69.71 (70.76)	60.89 (61.76)
East Asia						
PI	83.8	24.1	78 (117)	13.3 (20.7)	63.85 (64.38)	47.29 (47.34)
PD	288.9	21.3	92 (115)	22.4 (20.5)	64.03 (63.81)	47.66 (46.67)
2050A1B	300.0	19.8	87 (117)	22.9 (20.9)	60.90 (61.63)	46.88 (46.66)

ACPD
9, 4691–4725, 2009

Table 5. Radiative forcings in $W\,m^{-2}$ for past and future changes calculated using simulations that have AIE switched on (bracketed values are for simulations without AIE).

Climate forcing agent	Radiative forcing PD–PI	Radiative forcing 2050–PD
Ozone	+0.338 (+0.349)	+0.217 (+0.215)
Sulfate	−0.305 (−0.308)	−0.113 (−0.122)
BC	+0.313 (+0.324)	−0.091 (−0.097)
OC	−0.111 (−0.111)	+0.025 (+0.026)
Total Aerosol Direct	−0.103 (−0.095)	−0.179 (−0.193)
Aerosol Indirect Effect	−2.001	−0.601

ACPD
9, 4691–4725, 2009

Table 6. Global mean CH_4 lifetime (years) for each of the sensitivity simulations described in Table 2. The percentage change relative to the relevant present day simulation is indicated.

Simulation	Global annual mean CH_4 lifetime
Sim PI_AIE	8.53 (−11.5%)
Sim PD_AIE	9.64
Sim 2050_AIE	9.85 (+2.2%)
Sim PI	8.81 (−10.3%)
Sim PD	9.83
Sim 2050	9.99 (+1.6%)

ACPD
9, 4691–4725, 2009

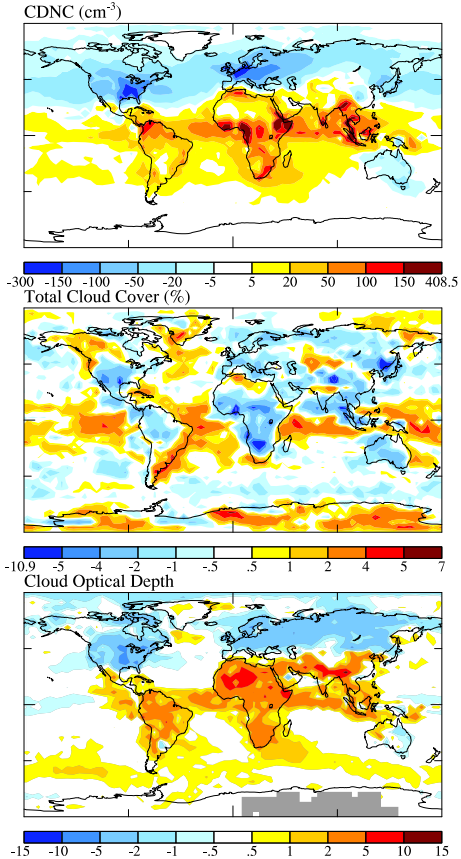

Fig. 1. Difference in annual average cloud droplet number concentration (CDNC) in cm^{-3}, total cloud cover in % and cloud optical depth (COD) for the future case (2050–PD).

ACPD
9, 4691–4725, 2009

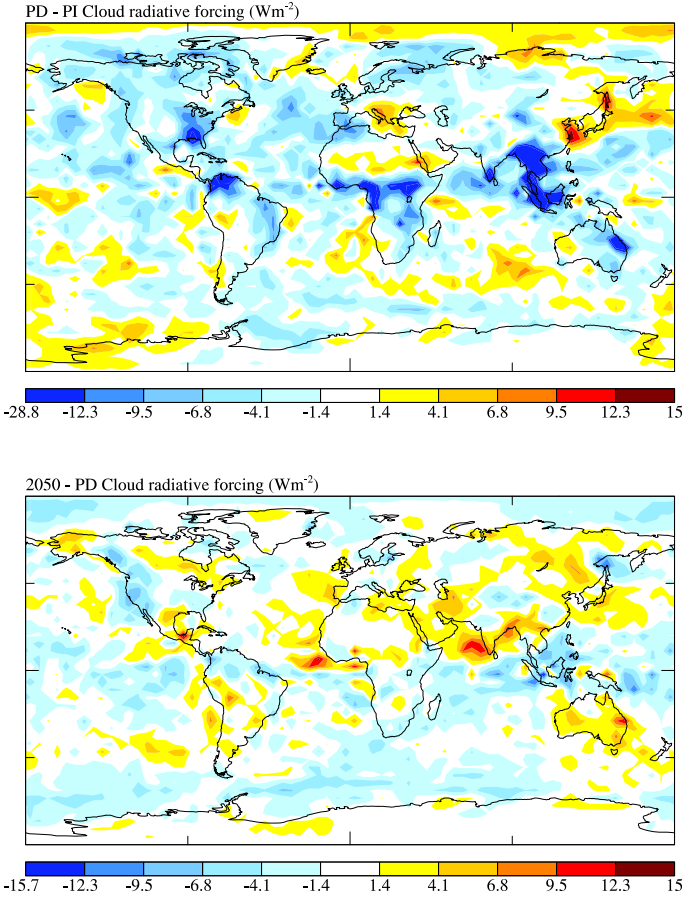

Fig. 2. Annual average cloud radiative forcing for PD–PI (top panel) and 2050–PD (bottom panel) in $W\,m^{-2}$.

ACPD
9, 4691–4725, 2009

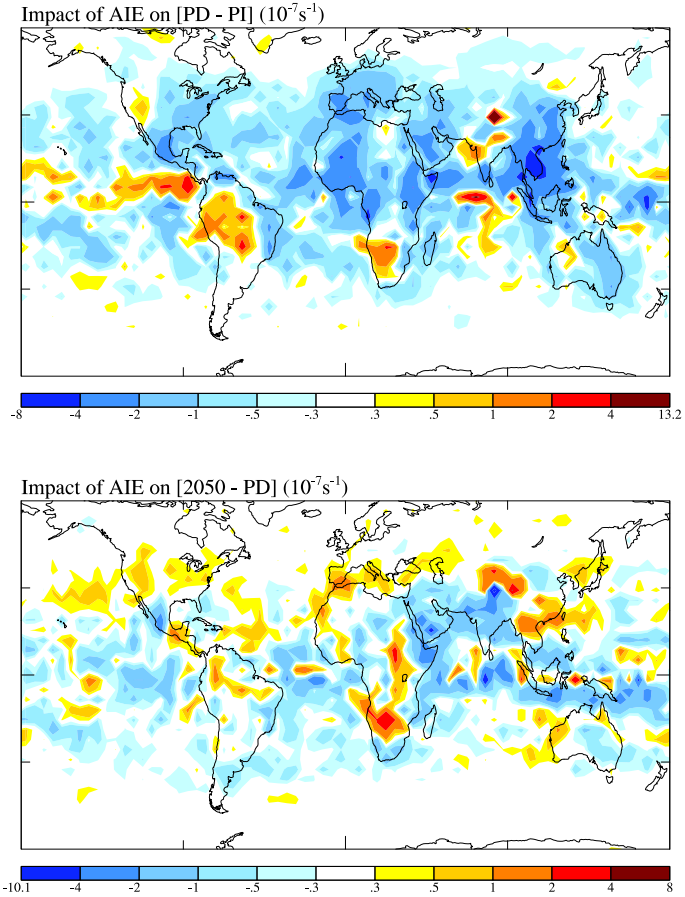

Fig. 3. Impact of AIE on the past (top panel) and future (bottom panel) changes in annual average photolysis rate $J(O^1D)$ in model surface layer in 10^{-7} s^{-1}.

ACPD
9, 4691–4725, 2009

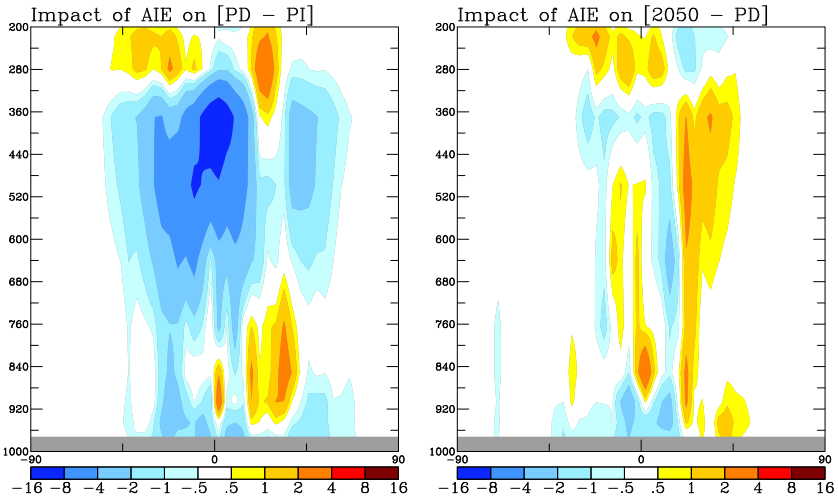

Fig. 4. Impact of AIE on the past (left panel) and future (right panel) changes in annual average zonal mean OH concentration in 10^4 molecule cm^{-3}.

ACPD
9, 4691–4725, 2009

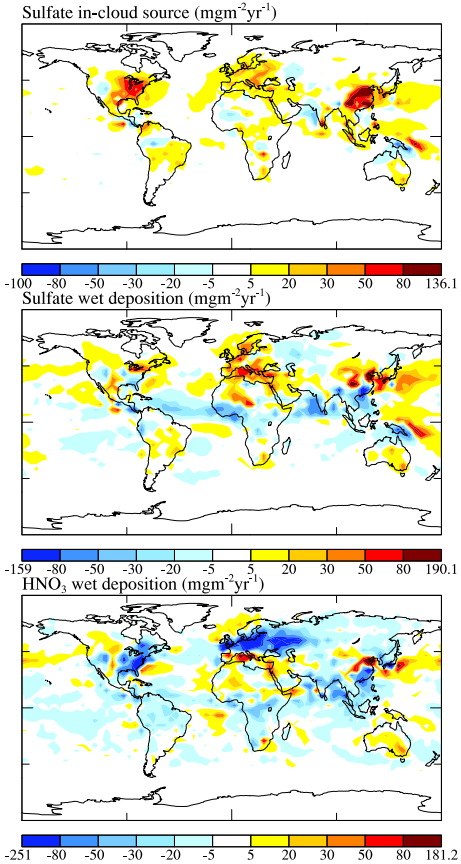

Fig. 5. Impact of AIE on the past change (PD–PI) in rates of sulfate in-cloud production, sulfate wet deposition and HNO_3 wet deposition in mg m^{-2} yr^{-1}.

ACPD
9, 4691–4725, 2009

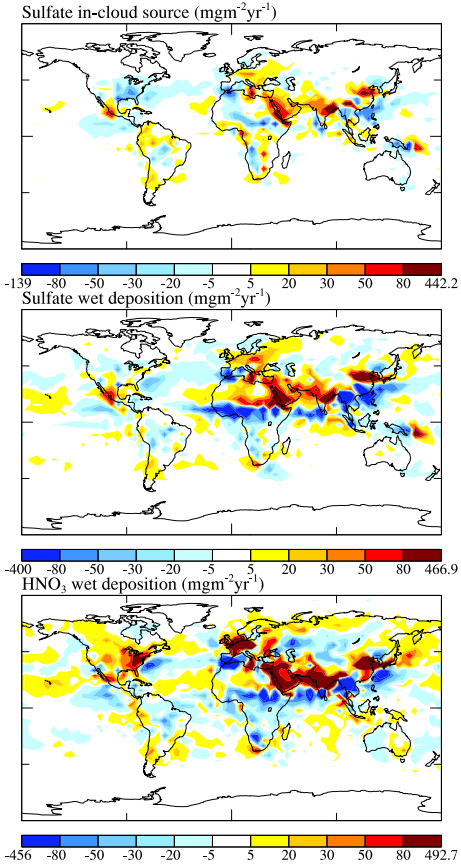

Fig. 6. Impact of AIE on the future change (2050–PD) in rates of sulfate in-cloud production, sulfate wet deposition and HNO_3 wet deposition in mg m^{-2} yr^{-1}.

ACPD
9, 4691–4725, 2009

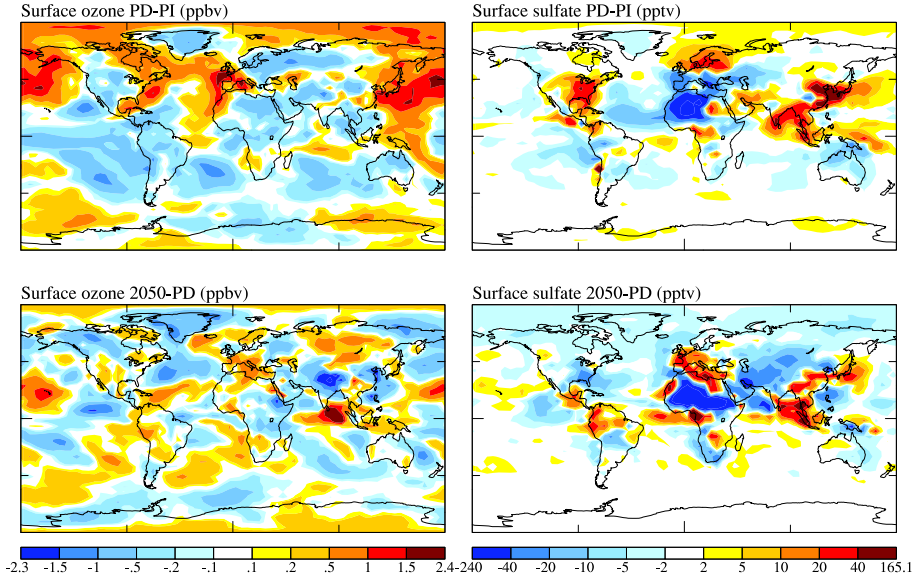

Fig. 7. Impact of AIE on past (PD–PI) and future (2050–PD) changes in surface O_3 and sulfate mixing ratios in ppbv and pptv, respectively.

ACPD
9, 4691–4725, 2009